# A new method for real radiation at next-to-next-to-leading order

Charalampos Anastasiou*
*Stanford Linear Accelerator Center, Stanford University, Stanford, California 94309, USA*

Kirill Melnikov†
*Department of Physics and Astronomy, University of Hawaii, 2505 Correa Rd., Honolulu, Hawaii 96822, USA*

Frank Petriello‡
*Department of Physics, Johns Hopkins University, 3400 North Charles St., Baltimore, Maryland 21218, USA*
(Received 2 December 2003; published 28 April 2004)

We propose a new method of computing real emission contributions to hard QCD processes. Our approach uses sector decomposition of the exclusive final-state phase space to enable extraction of all singularities of the real emission matrix elements before integration over any kinematic variable. The exact kinematics of the real emission process are preserved in all regions of phase space. Traditional approaches to extracting singularities from real emission matrix elements, such as phase space slicing and dipole subtraction, require both the determination of counterterms for double real emission amplitudes in singular kinematic limits and the integration of these contributions analytically to cancel the resulting singularities against virtual corrections. Our method addresses both of these issues. The implementation of constraints on the final-state phase space, including various jet algorithms, is simple using our approach. We illustrate our method using $e^+e^- \to$ jets at $O(\alpha_S^2)$ as an example.

DOI: 10.1103/PhysRevD.69.076010 PACS number(s): 11.15.Bt

## I. INTRODUCTION

The future high energy collider physics experimental program will measure phenomenologically interesting quantities with an unprecedented precision. To fully utilize these results, accurate theoretical predictions are required. In particular, the large value of the strong coupling constant $\alpha_S$ implies that perturbative QCD corrections through next-to-next-to-leading order (NNLO) in $\alpha_S$ are needed. The calculation of NNLO QCD corrections has advanced rapidly in the past few years. The progress has resulted primarily because of the realization that the computation of two-loop virtual corrections can be algorithmically structured and automated. These advances culminated in the evaluation of two-loop virtual corrections for $1 \to 3$ and all massless $2 \to 2$ scattering processes in perturbative QCD [1].

Unfortunately, these calculations have not yet produced improved theoretical predictions for many observables. The computation of infrared-safe quantities requires two additional ingredients: the real-virtual contributions, which denote the one-loop corrections to processes with one additional parton in the final state, and the real-real contributions, which denote tree-level processes with two additional partons in the final state. The two components of the real-virtual contributions, one-loop virtual corrections and single emission amplitudes, have both been well studied. However, the double emission corrections required for the real-real contributions are relatively unknown; the first steps towards understanding them have been taken only recently [3,4].

The current state-of-the-art can be illustrated using $e^+e^- \to 2$ jets as an example. Unresolved double real emission corrections appear for the first time at NNLO. The 2 jet cross section is currently computed at NNLO by taking the difference of the $O(\alpha_S^2)$ $e^+e^- \to$ hadrons cross section and the $e^+e^- \to 3$ and 4 jet results at NLO and LO, respectively. Only the total 2 jet cross section can be derived using this technique. All information concerning the invariant mass and angular distributions of the jets is lost.

The inability to compute the 2 jet cross section directly at NNLO arises from the poor understanding of the singular structure of the double real emission corrections. Infrared and collinear singularities cancel between virtual and real corrections only after integration over certain kinematic variables makes the $1/\epsilon$ poles in the real emission contributions explicit. However, since a primary goal of computing higher order QCD corrections to scattering processes is to produce Monte Carlo event generators that correctly describe the kinematics of each partonic event, only a restricted region of the final-state phase space can be integrated over. Only near the edges of the available phase space, where two or more partons become degenerate and combine to form a single jet, can the integration be performed without changing the kinematics of the final state. All singularities occur in these limits, and they can in principle be extracted and cancelled against those arising from virtual corrections. Unfortunately, these singularities overlap; this severely complicates their extraction.

The existing approaches to computing double real emission corrections extend methods used to handle single real emission amplitudes. There are two standard techniques for extracting single real emission singularities: phase space slicing [6,7] and dipole subtraction [8–10]. Extending these approaches to double real emission corrections requires two

*Email address: babis@slac.stanford.edu
†Email address: kirill@phys.hawaii.edu
‡Email address: frankp@pha.jhu.edu

 

non-trivial steps: a determination of the simplified matrix elements that approximate the complete double real emission amplitudes in singular kinematic regions, and an integration of these matrix elements over the unresolved regions of the multiparticle phase space. The difference of the exact and approximate matrix elements is by construction finite, and can be integrated numerically. The integration of the approximate matrix elements over the phase space boundaries produces the required $1/\epsilon$ poles that cancel against the virtual corrections. Both steps must be completed to obtain an NNLO prediction. Although some progress has recently been made [2–5], a functional method for calculating NNLO real emission corrections has not yet been demonstrated; a substantial effort is still required to obtain phenomenological results.

We present here a new approach to this problem. We illustrate our technique by considering the extraction of singularities from $1\to4$ processes, where the final state particles are massless. Our approach is based upon a few ideas. We first derive a factorized parametrization of the four particle phase space following a simple procedure. We, then, use sector decomposition [11–13] to separate the overlapping divergences which appear in the double real emission matrix elements. After this separation is performed, the phase space singularities can be extracted using standard expansions in terms of plus distributions. The processes of finding the required sectors and extracting the singularities are completely automated. The resulting matrix elements are finite and fully differential, and can be used to create NNLO Monte Carlo event generators. We discuss in some detail the example of $e^+e^-\to$ hadrons at $O(\alpha_S^2)$, which includes the 2 jet cross section at NNLO, the three jet cross section at NLO, and the 4 jet cross section at LO.

The paper is organized as follows. In Sec. II we introduce our method by considering $e^+e^-\to2$ jets at NLO and $e^+e^-\to3$ jets at the tree level. We begin our discussion of the 2 jet cross section at NNLO in Sec. III by describing our parametrization of the four-particle phase space. We also explain how we use sector decomposition to separate the overlapping singularities that appear in the matrix elements. In Sec. IV we apply our technique to the two most difficult interferences that appear in the double real emission contributions. After demonstrating that our method is powerful enough to handle the most complicated scenario, we apply it to a simple but realistic example in Sec. V: the $N_f$ dependent contribution to $e^+e^-\to$ hadrons at $O(\alpha_S^2)$. This process contributes to the 2 jet cross section at NNLO, the 3 jet cross section at NLO, and the 4 jet cross section at LO. Finally, we present our conclusions and discuss future prospects in Sec. VI.

## II. THE NLO EXAMPLE

We begin by considering the $O(\alpha_s)$ contribution to $e^+e^-\to$hadrons, which contains both the NLO correction to $e^+e^-\to2$ jets and the LO contribution to $e^+e^-\to3$ jets. Although many of the complexities of the NNLO case are absent in this calculation, it illustrates several important features of our method. At the partonic level, we must compute the one-loop virtual corrections to $e^+e^-\to q\bar{q}$ and the real emission process $e^+e^-\to q\bar{q}g$.

We consider first the real emission correction $e^+e^-\to q\bar{q}g$. The kinematics of the final state is fully described by the invariant masses $s_{q\bar{q}}, s_{qg}$, and $s_{\bar{q}g}$, which satisfy the constraint

$$s_{q\bar{q}}+s_{qg}+s_{\bar{q}g}=s. \tag{1}$$

Here, $s$ is the center of mass energy squared of the colliding electron and positron. The three particle phase space can be written as

$$\int [dq][d\bar{q}][dg](2\pi)^d\delta^{(d)}(p_1+p_2-q-\bar{q}-g)$$
$$=\frac{1}{(4\pi)^{d/2}}\frac{\mathcal{R}_2}{\Gamma(1-\epsilon)}s^{1-2\epsilon}\int_0^1 d\lambda_1 d\lambda_2\lambda_1^{-\epsilon}(1-\lambda_1)^{-\epsilon}\lambda_2^{-\epsilon}$$
$$\times(1-\lambda_2)^{1-2\epsilon}, \tag{2}$$

where $d=4-2\epsilon$, $[dk]=d^{d-1}k/(2\pi)^{d-1}k_0$, $\mathcal{R}_2$ is the integrated phase space of the two massless particles,

$$\mathcal{R}_2=\frac{1}{(2\pi)^{d-2}}\frac{\Omega_{d-1}}{2^{d-1}}, \tag{3}$$

and $\Omega_d$ is the solid angle in $d$ dimensions,

$$\Omega_d=\frac{2\pi^{d/2}}{\Gamma\left(\frac{d}{2}\right)}. \tag{4}$$

The invariant masses have the following expressions in terms of $\lambda_1$ and $\lambda_2$:

$$s_{q\bar{q}}=s(1-\lambda_2)(1-\lambda_1),\quad s_{qg}=s(1-\lambda_2)\lambda_1,\quad s_{\bar{q}g}=s\lambda_2. \tag{5}$$

In what follows we set $s=1$ for simplicity, and restore the correct dimensions in final results.

The matrix element for the $\gamma^*\to q\bar{q}g$ process is given by two diagrams. Upon squaring these and using the expressions for the invariant masses given in Eq. (5), we derive [6]

$$|\mathcal{M}|^2=\frac{32(1-\epsilon)}{\lambda_1\lambda_2(1-\lambda_2)}(2(1-\lambda_1)(1-\lambda_2)+\lambda_2^2+\lambda_1^2(1-\lambda_2)^2$$
$$-\epsilon[\lambda_1+\lambda_2-\lambda_1\lambda_2]^2). \tag{6}$$

After substituting the expression for the matrix element squared into the three-particle phase space, we arrive at the expression

$$\int_0^1 d\lambda_1 d\lambda_2 \frac{d^2\sigma_R}{d\lambda_1 d\lambda_2} = \frac{1}{(4\pi)^{d/2}} \frac{\mathcal{R}_2}{\Gamma(1-\epsilon)} \int_0^1 d\lambda_1 d\lambda_2 (\lambda_1\lambda_2)^{-\epsilon-1} \times (1-\lambda_1)^{-\epsilon}(1-\lambda_2)^{-2\epsilon} g(\lambda_1,\lambda_2), \tag{7}$$

where $g(\lambda_1,\lambda_2)$ is a nonsingular function of the $\lambda_i$. The phase space singularities in the above expression can be extracted before integration by using the standard decomposition in terms of plus distributions:

$$\lambda^{-1+\epsilon} = \frac{1}{\epsilon}\delta(\lambda) + \sum_{n=0}^{\infty} \frac{\epsilon^n}{n!}\left[\frac{\ln^n(\lambda)}{\lambda}\right]_+, \tag{8}$$

where a plus distribution is defined via

$$\int_0^1 d\lambda \left[\frac{\ln^n(\lambda)}{\lambda}\right]_+ f(\lambda) = \int_0^1 d\lambda \, \ln^n(\lambda)\left[\frac{f(\lambda)-f(0)}{\lambda}\right]. \tag{9}$$

Substituting this decomposition into Eq. (7), we derive the following expression for the real emission cross section:

$$\begin{aligned}\frac{d^2\sigma_R}{d\lambda_1 d\lambda_2} = \frac{64\pi\alpha_s}{3}\sigma_0 \frac{\Gamma(1+\epsilon)}{(4\pi)^{d/2}} \Bigg\{ & \frac{\delta(\lambda_1)\delta(\lambda_2)}{\epsilon^2} + \frac{1}{\epsilon}\left[ -\frac{\delta(\lambda_1)}{[\lambda_2]_+} - \frac{\delta(\lambda_2)}{[\lambda_1]_+} + \left(1-\frac{\lambda_1}{2}\right)\delta(\lambda_2) + \left(1-\frac{\lambda_2}{2}\right)\delta(\lambda_1) - \delta(\lambda_1)\delta(\lambda_2)\right] \\ & + \left(\lambda_1 - 1 + \frac{1}{2}\frac{(2-2\lambda_1+\lambda_1^2)\ln(1-\lambda_1)}{\lambda_1} - \left(1-\frac{\lambda_1}{2}\right)\ln(\lambda_1) + \left[\frac{1}{\lambda_1}\right]_+ + \left[\frac{\ln(\lambda_1)}{\lambda_1}\right]_+\right)\delta(\lambda_2) \\ & + \left(\lambda_2 - 1 + \frac{(2-2\lambda_2+\lambda_2^2)\ln(1-\lambda_2)}{\lambda_2} - \left(1-\frac{\lambda_2}{2}\right)\ln(\lambda_2) + \left[\frac{1}{\lambda_2}\right]_+ + \left[\frac{\ln(\lambda_2)}{\lambda_2}\right]_+\right)\delta(\lambda_1) \\ & - \left(1-\frac{\lambda_1}{2}\right)\left[\frac{1}{\lambda_2}\right]_+ - \left(1-\frac{\lambda_2}{2}\right)\left[\frac{1}{\lambda_1}\right]_+ + \left[\frac{1}{\lambda_1}\right]_+\left[\frac{1}{\lambda_2}\right]_+ - \frac{\pi^2}{6}\delta(\lambda_1)\delta(\lambda_2) + 1 - \lambda_1\left(1-\frac{\lambda_2}{2}\right)\Bigg\}. \end{aligned} \tag{10}$$

$\sigma_0$ is the tree level cross section for $e^+e^- \to q\bar{q}$: $\sigma_0 = 4\pi\alpha_{\rm EM}Q_q^2/s$. For the calculation of the NLO corrections to the 2 jet cross section we also require the virtual corrections to the $e^+e^- \to q\bar{q}$ process; we find [6]

$$\frac{d\sigma_V}{d\lambda_1 d\lambda_2} = \frac{64\pi\alpha_s}{3}\sigma_0 \frac{\Gamma(1+\epsilon)}{(4\pi)^{d/2}} \times \left\{ -\frac{1}{\epsilon^2} - \frac{1}{2\epsilon} + \frac{2\pi^2}{3} - \frac{5}{2}\right\}\delta(\lambda_1)\delta(\lambda_2). \tag{11}$$

We now discuss the calculation of the $n$ jet cross section; here, $n$ equals either 2 or 3. We introduce the jet function

$$F_J^{(n)}(s_{q\bar{q}}, s_{qg}, s_{\bar{q}g}) = F_J^{(n)}((1-\lambda_1)(1-\lambda_2), \lambda_1(1-\lambda_2), \lambda_2). \tag{12}$$

The $n$ jet cross section becomes

$$\sigma_J^{(n)} = \int_0^1 d\lambda_1 d\lambda_2 F_J^{(n)}(s_{ij}) \left\{ \sigma_o \delta(\lambda_1)\delta(\lambda_2) + \frac{d\sigma_V}{d\lambda_1 d\lambda_2} + \frac{d\sigma_R}{d\lambda_1 d\lambda_2}\right\}. \tag{13}$$

It is clear from the expressions in Eqs. (10) and (11) that the $1/\epsilon^2$ poles cancel when $\sigma_V$ and $\sigma_R$ are combined. The $1/\epsilon$ poles in $\sigma_R$ require that either $\lambda_1$ or $\lambda_2$ vanish. The jet function becomes either $F_J^{(n)}(s_{q\bar{q}}, s_{qg}, 0)$ or $F_J^{(n)}(s_{q\bar{q}}, 0, s_{\bar{q}g})$ in these cases, i.e., a 2 jet configuration is always obtained. The $1/\epsilon$ poles of both $\sigma_V$ and $\sigma_R$ occur in the 2 jet cross section; they cancel after integrating over $\lambda_1$ and $\lambda_2$, as required for infrared safe observables. Dropping the poles in $\epsilon$, we can write the $n$ jet cross section as an integral over the finite component of the partonic cross sections:

$$\sigma_J^{(n)} = \int_0^1 d\lambda_1 d\lambda_2 F_J^{(n)}(s_{ij}) \sigma_{finite}. \tag{14}$$

It is straightforward to check that this correctly reproduces known 2 and 3 jet cross sections for standard jet functions [14].

Several important aspects of this result generalize immediately to NNLO calculations. We were able to extract the singularities in $\epsilon$ without performing any integrations. The cancellation of the poles in $\epsilon$ can be checked numerically, and these terms can then be discarded. We note that by casting the subtraction operations needed for extracting the $\epsilon$ poles in terms of plus distributions, we have gained the flexibility to combine our result with any jet function and with any constraint on an infrared safe differential quantity. This greatly simplifies the calculation of NNLO cross sections.

## III. FOUR PARTICLE PHASE SPACE: PARAMETRIZATION AND SECTOR DECOMPOSITION

We present here our parametrization of the four particle phase space. After deriving the relevant formulas, we discuss the complications that arise when we attempt to extract phase space singularities using the method discussed in the previous section. We show how sector decomposition of the phase space solves these problems, and apply the technique to a few examples.

We begin with the following expression for the four particle phase space:

$$\mathcal{I}_4=\int [dp_1][d\overline{p_2}][dp_3][dp_4](2\pi)^d \times \delta^{(d)}(p-p_1-p_2-p_3-p_4). \quad (15)$$

This phase space is described by five independent invariant masses. A convenient set is $\{s_{134},s_{234},s_{34},s_{13},s_{24}\}$, where $s_{ij}=(p_i+p_j)^2$ and $s_{ijk}=(p_i+p_j+p_k)^2$. We split the above integral into three subintegrals:

$$\mathcal{I}_4=\left(\frac{1}{2\pi}\right)^{3d-4}\int ds_{234}ds_{34}ds_{134}ds_{23}ds_{13}I_1I_2I_3, \quad (16)$$

where

$$I_1=\int d^dp_1d^dQ_{234}\delta^{(d)}(p-p_1-Q_{234})\delta(p_1^2)\delta(Q_{234}^2-s_{234}), \quad (17)$$

$$I_2=\int d^dp_2d^dQ_{34}\delta^{(d)}(Q_{234}-p_2-Q_{34})\delta(p_2^2)\delta(Q_{34}^2-s_{34}), \quad (18)$$

and

$$I_3=\int d^dp_3d^dp_4\delta^{(d)}(Q_{34}-p_3-p_4)\delta(p_3^2)\delta(p_4^2). \quad (19)$$

We now constrain the integrations over the $s_{ij}$ by introducing the following delta functions into $\mathcal{I}_4$:

$$\delta(s_{234}-Q_{234}^2)\delta(s_{34}-Q_{34}^2)\delta(s_{134}-Q_{134}^2) \times \delta(s_{23}-2p_2\cdot p_3)\delta(s_{13}-2p_1\cdot p_3). \quad (20)$$

To derive representations of these integrals from which the phase space singularities can be conveniently extracted, we bring the limits of integration for each integral from 0 to 1 using transformations of the form $s_{ij}=\lambda_i(s_{ij}^+-s_{ij}^-)+s_{ij}^-$, where $s_{ij}^\pm$ denote the maximum and minimum values of the corresponding invariant masses. Using the delta functions to simplify the integrations, performing the transformation to the variables $\lambda_i$, and including the Jacobian $|\partial s_{ij}/\partial\lambda_k|$, we arrive at

$$\begin{aligned}\mathcal{I}_4=\mathcal{N}_4\int_0^1 &d\lambda_1d\lambda_2d\lambda_3d\lambda_4d\lambda_5\delta(\lambda_1-\lambda_1')\\ &\times\delta(\lambda_2-\lambda_2')\delta(\lambda_3-\lambda_3')\delta(\lambda_4-\lambda_4')\delta(\lambda_5-\lambda_5')\\ &\times[\lambda_1(1-\lambda_1)(1-\lambda_2)]^{1-2\epsilon}\\ &\times[\lambda_2\lambda_3(1-\lambda_3)\lambda_4(1-\lambda_4)]^{-\epsilon}\\ &\times[\lambda_5(1-\lambda_5)]^{-1/2-\epsilon}. \end{aligned} \quad (21)$$

We have extracted the overall normalization

$$\mathcal{N}_4=\mathcal{R}_2\left[\frac{\Gamma(1+\epsilon)}{(4\pi)^{d/2}}\right]^2\left[\frac{\Omega_{d-1}}{2^{d-1}}\right]^2\frac{(4\pi)^d}{(2\pi)^{2d-2}} \times\frac{\Gamma^2(2-2\epsilon)\Gamma(1-2\epsilon)}{\Gamma^2(1+\epsilon)\Gamma^4(1-\epsilon)\Gamma^2(1/2-\epsilon)}. \quad (22)$$

The invariant masses have the following expressions in terms of the $\lambda_i$ (with $s=1$):

$$\begin{aligned} s_{234}&=\lambda_1,\\ s_{34}&=\lambda_1\lambda_2,\\ s_{23}&=\lambda_1(1-\lambda_2)\lambda_4,\\ s_{134}&=\lambda_2+\lambda_3(1-\lambda_1)(1-\lambda_2),\\ s_{13}&=\lambda_5(s_{13}^+-s_{13}^-)+s_{13}^-, \end{aligned} \quad (23)$$

with

$$s_{13}^\pm=(1-\lambda_1)[\lambda_3\lambda_4+\lambda_2(1-\lambda_3)(1-\lambda_4) \pm 2\sqrt{\lambda_2\lambda_3(1-\lambda_3)\lambda_4(1-\lambda_4)}]. \quad (24)$$

Difficulties arise when we substitute the matrix elements into the four particle phase space and attempt to expand the expression using Eq. (8). We will discuss in Sec. V the $N_f$ contributions to $e^+e^-\to 2$ jets; the matrix elements for the double real emission contribution to this process contain denominators of the form $1/s_{34}s_{234}s_{134}$. Using Eq. (23), this becomes

$$\frac{1}{s_{34}s_{234}s_{134}}=\frac{1}{\lambda_1^2\lambda_2[\lambda_2+\lambda_3(1-\lambda_1)(1-\lambda_2)]}. \quad (25)$$

The third term in this denominator is singular when e.g. both $\lambda_2,\lambda_3\to 0$, but not when only one does. If we combine the denominator with the integration measure in Eq. (21), and attempt to naively expand $\lambda_2^{-1-\epsilon}\to-\delta(\lambda_2)/\epsilon+\cdots$, $\lambda_3^{-\epsilon}\to 1-\epsilon\ln(\lambda_3)+\cdots$, we will find unregulated singularities as $\lambda_3\to 0$. The most convenient method for separating the overlapping singularities in $\lambda_2$ and $\lambda_3$ is sector decomposition [11–13]. To illustrate this technique, a simple example suffices. We consider the integral

$$I=\int_0^1 dxdyx^{-1-\epsilon}y^{-1-\epsilon}(x+y)^{-\epsilon}. \tag{26}$$

The $1/x$ and $1/y$ factors cannot be expanded in plus distributions, as the logarithms from the expansion of $x+y$ will produce singular terms. We split this integral into two parts,

$$I_1=\int_0^1 dx\int_0^x dyx^{-1-\epsilon}y^{-1-\epsilon}(x+y)^{-\epsilon},$$

$$I_2=\int_0^1 dy\int_0^y dxx^{-1-\epsilon}y^{-1-\epsilon}(x+y)^{-\epsilon}. \tag{27}$$

In $I_1$ we set $y'=y/x$, and in $I_2$ we set $x'=x/y$. Performing these variable changes, we find

$$I_1=\int_0^1 dxdyx^{-1-3\epsilon}y^{-1-\epsilon}(1+y)^{-\epsilon},$$

$$I_2=\int_0^1 dxdyy^{-1-3\epsilon}x^{-1-\epsilon}(1+x)^{-\epsilon}. \tag{28}$$

The singularities in $x$ and $y$ are now separated in each integral, and can be extracted using Eq. (8).

One great advantage of this technique is the ease with which it can be automated. The rules to determine when a term requires sector decomposition are simple; if the expression becomes singular when two (or more) variables $x,y\to 0$, but remains finite when either $x\to 0$ or $y\to 0$, then the transformations discussed below Eq. (27) should be performed. Another advantage of sector decomposition is that it can be applied to fractional powers in addition to denominators, as illustrated in the example above.

We now discuss the application of this method to the denominator in Eq. (25), to show how it works in practice. It is convenient to first separate the two singularities that can occur if $x\to 0$ or $x\to 1$ by splitting the integration as

$$\int_0^1 dx\to\int_0^{1/2} dx+\int_{1/2}^1 dx, \tag{29}$$

and changing $x\to x'$ in the second integration so that $x=1$ is mapped to $x'=0$. Doing so for the three variables $\lambda_1$, $\lambda_2$, and $\lambda_3$ produces eight sectors. We focus on the sector where originally $\lambda_1,\lambda_2,\lambda_3<1/2$. The denominator has the form

$$\mathcal{D}=\frac{1}{\lambda_1^2\lambda_2\left[\lambda_2+\lambda_3\left(1-\frac{\lambda_1}{2}\right)\left(1-\frac{\lambda_2}{2}\right)\right]}. \tag{30}$$

We now perform a sector decomposition in the variables $\lambda_2$ and $\lambda_3$, using the transformations given below equation Eq. (27): in sector $a$ we set $\lambda_2\to\lambda_2\lambda_3$, and in sector $b$ we set $\lambda_3\to\lambda_3\lambda_2$. Combining the Jacobian of the variable change with the denominator, we find the following expressions in each sector:

$$\mathcal{D}^a=\frac{1}{\lambda_1^2\lambda_2\lambda_3\left[\lambda_2+\left(1-\frac{\lambda_1}{2}\right)\left(1-\frac{\lambda_2\lambda_3}{2}\right)\right]},$$

$$D^b=\frac{1}{\lambda_1^2\lambda_2\left[1+\lambda_3\left(1-\frac{\lambda_1}{2}\right)\left(1-\frac{\lambda_2}{2}\right)\right]}. \tag{31}$$

The terms in brackets are now finite in all limits; the denominators can be combined with the phase space measure, and the standard decomposition in plus distributions can be used to extract singularities. Note that the above transformations must also be performed in the integration measure. After splitting the integration as in Eq. (29), the measure contains terms of the form $(1-\lambda_i/2)$. After sector decomposition, these become $(1-\lambda_i\lambda_j/2)$. If we had not performed this split, we would have produced terms of the form $(1-\lambda_i\lambda_j)$. These are potentially singular when $\lambda_i,\lambda_j\to 1$, and would require further sector decomposition.

We must discuss two subtleties that can occur when using the method presented above. The representation of $\mathcal{I}_4$ we have derived is convenient for expressions that do not contain $s_{13}$ or $s_{14}$ [see Eq. (23)] in the denominator. In such terms, it is difficult to extract singularities in $\lambda_2,\lambda_3,\lambda_4$ that appear after integrating over $\lambda_5$. One can always remap the momenta of the final state particles in a given diagram in such a way that $s_{14}$ never appears in the denominator. For those terms that contain $s_{13}$, we first bring the limits of the $s_{13}$ integration from 0 to 1 using the transformation

$$\hat{\lambda}_5=\frac{s_{13}-s_{13}^-}{s_{13}^+-s_{13}^-}\frac{s_{13}^+}{s_{13}}. \tag{32}$$

We then derive the following expression for the four particle phase space:

$$\begin{aligned}\hat{\mathcal{I}}_4=\mathcal{N}_4\int_0^1 &d\lambda_1 d\lambda_2 d\lambda_3 d\lambda_4 d\hat{\lambda}_5\,\delta(\lambda_1-\lambda_1')\,\delta(\lambda_2-\lambda_2')\\ &\times\delta(\lambda_3-\lambda_3')\,\delta(\lambda_4-\lambda_4')\,\delta(\hat{\lambda}_5-\hat{\lambda}_5')\\ &\times[\lambda_1(1-\lambda_1)(1-\lambda_2)]^{1-2e}\\ &\times[\lambda_2\lambda_3(1-\lambda_3)\lambda_4(1-\lambda_4)]^{-\epsilon}[\hat{\lambda}_5(1-\hat{\lambda}_5)]^{-1/2-\epsilon}\\ &\times s_{13}(\hat{\lambda}_5)[s_{13}^+s_{13}^-]^{-1/2-\epsilon}\\ &\times\{(1-\hat{\lambda}_5)(s_{13}^+-s_{13}^-)+s_{13}^-\}^{2\epsilon}.\end{aligned} \tag{33}$$

Factors of $s_{13}$ that appear in the denominator are cancelled by the Jacobian of the nonlinear transformation of Eq. (32), and the remaining $\hat{\lambda}_5$ integration does not produce dangerous singularities. Therefore, sector decomposition of the $\hat{\lambda}_5$ integration is never required.

One further complication exists. Using the expressions in Eq. (24), we find

$$[s_{13}^{+}s_{13}^{-}]^{-1/2-\epsilon}=(1-\lambda_1)^{-1-2\epsilon}|\lambda_2(1-\lambda_3)\times(1-\lambda_4)-\lambda_3\lambda_4|^{-1-2\epsilon}. \quad (34)$$

This expression is singular on a manifold of points in the interior of the phase space. We wish to move these singularities to the boundary of the integration region. To do so, we first note that the singularity occurs when

$$\lambda_4\to\lambda_4^s=\frac{\lambda_2(1-\lambda_3)}{\lambda_3+\lambda_2(1-\lambda_3)}; \quad (35)$$

this value is always in the integration region. We can therefore split the $\lambda_4$ integration into two parts,

$$\int_0^1 d\lambda_4=\int_0^{\lambda_4^s} d\lambda_4+\int_{\lambda_4^s}^1 d\lambda_4, \quad (36)$$

and then bring the integration limits back to 0 and 1. Doing so produces two integrals, $\hat{\mathcal{I}}_4^a$ and $\hat{\mathcal{I}}_4^b$, with all singularities moved to the boundaries of the integration regions; these can be extracted using the sector decomposition technique discussed above.

To summarize, we derive analytic results for the double-real radiation corrections by following these steps:

We derive a factorized parametrization of the $1\to4$ phase-space as in Eq. (21) or Eq. (33), in terms of kinematic variables which range from 0 to 1.

We remove singularities from inside the allowed phase-space region to the boundaries by splitting appropriately the integrations and mapping them back to the $[0,1]$ interval.

We then apply sector decomposition to disentangle the overlapping singularities.

Finally, we extract the $\epsilon$ poles in terms of plus distributions.

## IV. THE UNITARITY CHECK

Having discussed the four particle phase space and the technique of sector decomposition, we now illustrate our method by considering two examples of double real emission integrals with four propagators. These are the most complicated phase space integrals that appear in $1\to4$ processes. We check our calculation of the double real emission corrections using their contributions to the imaginary parts of three-loop propagator diagrams. From the optical theorem we know that the imaginary parts of such diagrams are given by the sum of all cuts, where all possible combinations of internal propagators are put on-shell. The required cuts also include real-virtual and virtual-virtual ones. These are simple to compute, as are the imaginary parts of the propagator diagrams. We can therefore derive analytic expressions for the real-real cuts, which we can compare with the results we obtain using the methods presented in the previous sections. The checks we perform in this section involve inclusive integrations over the real emission phase space, in order to compare with the imaginary part of the relevant propagator diagrams. We will demonstrate in the next section that the implementation of jet functions into our method is simple in both principle and practice.

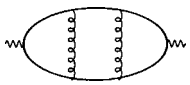

FIG. 1. A planar propagator-type diagram contributing to the $e^+e^-$ cross section at NNLO.

We begin by considering the maximally planar propagator integrals which arise from Feynman graphs as the one shown in Fig. 1. The sum of all cuts for these diagrams contributes to the $e^+e^-$ total cross section. Here, we examine the underlying scalar integral of these diagrams after we set their numerator to one. The analytic expression for this integral can be found using MINCER [15]; it is finite, and therefore its imaginary part vanishes. The sum of all possible cuts of this diagram must also vanish. This diagram has three distinct virtual-virtual cuts: the interference of a two-loop planar vertex correction to $\gamma^*\to q\bar{q}$ with the tree level contribution diagram together with its complex conjugate, and the square of the one-loop vertex correction to this process. It has four real-virtual cuts: two copies of the tree-level contribution to $\gamma^*\to q\bar{q}g$ interfered with the vertex correction to this process with the gluon radiated off the opposite quark leg, and two copies of its complex conjugate. Finally, it has two real-real cuts: the tree-level contribution to $\gamma^*\to q\bar{q}gg$ with both gluons radiated from a single quark line interfered with the diagram where both gluons are radiated from the opposite quark line, together with the complex conjugate of this contribution.

The first virtual-virtual term, the two-loop vertex correction and its complex conjugate, is [16]

$$V_p=\left(\frac{\Gamma(1+\epsilon)}{(4\pi)^{d/2}}\right)^2\mathcal{R}_2\left(\frac{1}{2\epsilon^4}-\frac{4\zeta_2}{\epsilon^2}+\frac{10\zeta_3}{\epsilon}-\frac{38\zeta_2^2}{5}\right), \quad (37)$$

where $\mathcal{R}_2$ is the two-particle phase space introduced in Sec. II. The second virtual-virtual contribution, the square of the one-loop vertex correction, is

$$V_p^{1l}=\left(\frac{\Gamma(1+\epsilon)}{(4\pi)^{d/2}}\right)^2\mathcal{R}_2\left(\frac{1}{\epsilon^4}-\frac{2\zeta_2}{\epsilon^2}-\frac{4\zeta_3}{\epsilon}-\frac{4\zeta_2^2}{5}\right). \quad (38)$$

The four real-virtual contributions give

$$RV_p=\left(\frac{\Gamma(1+\epsilon)}{(4\pi)^{d/2}}\right)^2\mathcal{R}_2\left(\frac{-2}{\epsilon^4}+\frac{8\zeta_2}{\epsilon^2}-\frac{20\zeta_3}{\epsilon}-\frac{156\zeta_2^2}{5}\right). \quad (39)$$

The sum of the above contributions with a minus sign should equal the sum of the real-real cuts of this diagram. We obtain

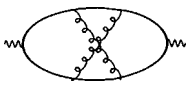

FIG. 2. A nonplanar propagator-type diagram contributing to the $e^+e^-$ cross section at NNLO.

$$R_p = \left(\frac{\Gamma(1+\epsilon)}{(4\pi)^{d/2}}\right)^2 \mathcal{R}_2\left(\frac{1}{2\epsilon^4} - \frac{2\zeta_2}{\epsilon^2} + \frac{14\zeta_3}{\epsilon} + \frac{198\zeta_2^2}{5}\right)$$
$$= \left(\frac{\Gamma(1+\epsilon)}{(4\pi)^{d/2}}\right)^2 \mathcal{R}_2\left(\frac{0.5}{\epsilon^4} - \frac{3.2899}{\epsilon^2} + \frac{16.829}{\epsilon} + 107.15\right). \tag{40}$$

In terms of the invariant masses introduced in the previous section, this contribution should be equal to

$$R_p^{\rm num} = 2\left\langle \frac{1}{s_{13}s_{134}s_{24}s_{243}}\right\rangle, \tag{41}$$

where the factor of two indicates the sum of both real-real cuts. This integral involves the invariant mass $s_{13}$; its calculation therefore requires extensive use of sector decomposition and the reparametrization $\lambda_5 \to \hat{\lambda}_5$ discussed in the previous section. Using these techniques, and numerically integrating the result using VEGAS [17], we obtain

$$R_p^{\rm num} = \left(\frac{\Gamma(1+\epsilon)}{(4\pi)^{d/2}}\right)^2 \mathcal{R}_2\left(\frac{0.5}{\epsilon^4} + \frac{(-0.8\pm 9.2)\times 10^{-5}}{\epsilon^3} - \frac{3.2909\pm 0.0018}{\epsilon^2} + \frac{16.827\pm 0.010}{\epsilon} + 107.12\pm 0.07\right). \tag{42}$$

We have included the VEGAS errors for those terms which require nontrivial integrations. The agreement between the analytic and the numerical results is better than 0.1% for all terms considered, and the differences are consistent with the integration errors.

We now consider the nonplanar topologies shown in Fig. 2. Once again we focus on the scalar integral which is obtained from these topologies by setting their numerator to unity. The imaginary part of this integral vanishes; therefore, we can again verify our calculation of the double real emission contribution using sector decomposition by checking the cancellation of all possible cuts. This diagram has two virtual-virtual cuts: the interference of the two-loop nonplanar vertex correction with the tree level $\gamma^* \to q\bar{q}$ diagram, and its complex conjugate. It has four real-virtual cuts, each of which involves the one-loop box correction to $\gamma^* \to q\bar{q}g$ interfered with the tree-level contribution. Finally, it has five real-real cuts, of three distinct types: two cuts involving the emission of two gluons off a single quark line interfered with the emission of two gluons off the opposite quark line; two cuts where a radiated gluon splits into a $q\bar{q}$ pair; one cut where a gluon is radiated from each quark line. Since we are considering only scalar diagrams, the first four cuts give identical answers.

The virtual-virtual cuts sum to [16]

$$V_{np} = \left(\frac{\Gamma(1+\epsilon)}{(4\pi)^{d/2}}\right)^2 \mathcal{R}_2\left(\frac{2}{\epsilon^4} - \frac{38\zeta_2}{\epsilon^2} - \frac{54\zeta_3}{\epsilon} + \frac{966\zeta_2^2}{5}\right). \tag{43}$$

The real-virtual contribution involves the integration of the one-loop box diagram with one leg off-shell. There are two distinct ways of computing this diagram: either analytically using e.g. a Mellin-Barnes representation, or numerically using sector decomposition in a fashion identical to our approach to the real-real terms. The second method is particularly convenient, as it allows restrictions on the final-state phase space to be imposed easily. We now illustrate this technique.

The expression for the one-loop scalar box diagram with one external leg off-shell, valid to all orders in $\epsilon$, is

$$B = \frac{2}{\epsilon^2(4\pi)^{d/2}} \frac{\Gamma(1-\epsilon)^2\Gamma(1+\epsilon)}{\Gamma(1-2\epsilon)} \frac{1}{st} \times \left[ (-t)^{-\epsilon} F_{21}\left(1,-\epsilon,1-\epsilon,-\frac{u}{s}\right) + (-s)^{-\epsilon} F_{21}\left(1,-\epsilon,1-\epsilon,-\frac{u}{t}\right) - (-M^2)^{-\epsilon} F_{21}\left(1,-\epsilon,1-\epsilon,-\frac{M^2 u}{st}\right)\right]. \tag{44}$$

Here, $M^2$ is the virtuality of the off-shell leg, and $s,t,u$ are the usual Mandelstam variables. We set $M^2=1$ in what follows and choose the Mandelstam variables to be $s = s_{q\bar{q}} = \lambda_2$, $t = s_{\bar{q}g} = (1-\lambda_2)\lambda_1$, $u = s_{\bar{q}g} = (1-\lambda_2)(1-\lambda_1)$, where we have used our notation from Sec. II. The expression in Eq. (44) must be integrated over the three particle phase, together with an additional propagator $1/s_{\bar{q}g}$ coming from the interference with the tree-level diagram, and the three-particle phase space in Eq. (2). It is convenient to proceed in the following way. Using the integral representation for the hypergeometric function,

$$F_{21}(1,-\epsilon,1-\epsilon,z) = \frac{\Gamma(1-\epsilon)}{\Gamma(-\epsilon)} \int_0^1 dt \frac{t^{-\epsilon-1}}{1-tz}, \tag{45}$$

we can write the required integrals over the phase space and the auxiliary variable $t$ in a form that is directly amenable to sector decomposition. It is then a simple task to numerically compute the expansion of the real-virtual corrections in powers of $\epsilon$ using the techniques described above. The analytic result for the real-virtual cut was derived for the purpose of checking our calculation based on sector decomposition; summing the four cuts, we obtain

$$RV_{np}=\left(\frac{\Gamma(1+\epsilon)}{(4\pi)^{d/2}}\right)^2 \times\mathcal{R}_2\left(-\frac{10}{\epsilon^4}+\frac{128\zeta_2}{\epsilon^2}+\frac{356\zeta_3}{\epsilon}-\frac{1108\zeta_2^2}{5}\right). \tag{46}$$

Requiring the cancellation of all cuts, we derive the following analytic expression for the real-real contribution:

$$R_{np}=\left(\frac{\Gamma(1+\epsilon)}{(4\pi)^{d/2}}\right)^2\mathcal{R}_2\left(\frac{8}{\epsilon^4}-\frac{90\zeta_2}{\epsilon^2}-\frac{302\zeta_3}{\epsilon}+\frac{142\zeta_2^2}{5}\right) =\left(\frac{\Gamma(1+\epsilon)}{(4\pi)^{d/2}}\right)^2\mathcal{R}_2\left(\frac{8}{\epsilon^4}-\frac{148.04}{\epsilon^2}-\frac{363.02}{\epsilon}+76.84\right). \tag{47}$$

This result should be equal to the following sum of real-real integrals:

$$R_{np}^{\rm num}=\left\langle\frac{1}{s_{13}s_{12}s_{24}s_{34}}\right\rangle+4\left\langle\frac{1}{s_{13}s_{134}s_{23}s_{234}}\right\rangle. \tag{48}$$

Computing the above integrals using sector decomposition, we obtain

$$R=\left(\frac{\Gamma(1+\epsilon)}{(4\pi)^{d/2}}\right)^2\mathcal{R}_2\left(\frac{8}{\epsilon^4}-\frac{(5.8\pm6.4)\times10^{-4}}{\epsilon^3} -\frac{148.06\pm0.03}{\epsilon^2}-\frac{363.03\pm0.07}{\epsilon}+77.1\pm0.4\right). \tag{49}$$

The result found using sector decomposition is again consistent with that found by demanding the cancellation of all cuts, although the numerical precision of the finite piece is slightly worse. This can be improved with a more sophisticated numerical integration technique.

We therefore conclude that our method can accommodate the most difficult real-real phase space integrals needed for $1\to4$ processes. We next consider in detail the $N_f$ dependent contributions to the $e^+e^-\to2$, 3, and 4 jet cross sections. This example addresses the two remaining issues we must confront to fully validate our method: that jet functions can be implemented simply, and that bookkeeping of the sectors (i.e., the expressions for the $s_{ij}$ in each sector as a function of the rescaled $\lambda_i$) can be performed.

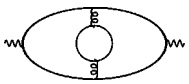

FIG. 3. An example of an $N_f$ dependent diagram at NNLO.

## V. $N_f$ DEPENDENT CONTRIBUTION TO $e^+e^-\to$2,3,4 jets

In this section we illustrate our method in a realistic NNLO example. We compute the $N_f$ dependent contributions to the 2 jet cross section at NNLO. When we wish to compute jet cross sections, we must include in our matrix elements a jet function, denoted by $F_J$ in Sec. II, that determines whether a given configuration contains 2, 3, or 4 jets. This function takes the invariant masses of all partonic pairs as its arguments. After splitting our result for the double real emission contribution into sectors, the invariant masses take different forms in terms of the $\lambda_i$ in each sector. This presents bookkeeping issues that must be addressed. We prove here that we can handle this problem by considering a realistic example. Taken in conjunction with the calculation in the previous section of the most difficult integrals that appear in $e^+e^-\to2$ jets, the reader should be convinced of the power of our approach.

An example of the diagrams that contribute to the $N_f$ dependent terms of $e^+e^-\to$ jets at $O(\alpha_S^2)$ is shown in Fig. 3. This diagram, together with the remaining contributions where the internal bubble is attached to a single quark line, contains both virtual-virtual and real-real cuts. At $O(\alpha_S^2)$ we must also consider the coupling constant renormalization of the $O(\alpha_S)$ result. To present numerical results we must also choose a jet algorithm; we use the JADE algorithm, with a separation parameter $y=0.1$.

The virtual correction only contributes to the two-jet configuration. Therefore, we write

$$\frac{\sigma_V}{\sigma_0}=\delta_{j,2}N_f\left(\frac{\alpha_s}{\pi}\right)^2\left(\frac{1}{18\epsilon^3}+\frac{11}{54\epsilon^2}+\frac{1}{\epsilon}\left(-\frac{11}{18}\zeta_2+\frac{269}{324}\right) +\frac{5423}{1944}-\frac{13}{27}\zeta_3-\frac{121}{54}\zeta_2\right), \tag{50}$$

where the Kronecker delta indicates the restriction to the 2 jet cross section. We compute the double real emission using the approach described in the previous sections, and extract the singularities prior to integration over any kinematic variables. Implementing the jet algorithm and performing the integrations over the five-dimensional phase space numerically, we obtain

$$\frac{\sigma_R}{\sigma_0}=N_f\left(\frac{\alpha_s}{\pi}\right)^2\left(\delta_{j,2}\left[-\frac{(5.5553\pm0.0005)\times10^{-2}}{\epsilon^3}-\frac{0.20369\pm0.00005}{\epsilon^2}+\frac{0.4180\pm0.0005}{\epsilon}+4.808\pm0.003\right] -\delta_{j,3}\left(\frac{0.41005\pm0.00016}{\epsilon}+2.9377\pm0.0018\right)+(1.4561\pm0.0018)\times10^{-3}\delta_{j,4}\right). \tag{51}$$

The $O(\alpha_s)$ cross section combines the virtual correction and the single real emission. We need this contribution to $O(\epsilon)$ to derive its contribution to the NNLO cross section. Using the results in Sec. II, we derive

$$\frac{\sigma^{(1)}}{\sigma_0}=\left(\frac{\alpha_s}{\pi}\right)N_f([-1.4597\pm 0.0013-(9.242\pm 0.004)\ \ \epsilon]\delta_{j,2} +[2.4575\pm 0.0012+(6.115\pm 0.003)\ \ \epsilon]\delta_{j,3}). \quad (52)$$

The $O(\alpha_s^2)$ contribution to the $e^+e^-$ annihilation into hadrons is then written as

$$\sigma^{(2)}=\sigma_V+\sigma_R-\frac{\beta_0}{\epsilon}\left(\frac{\alpha_s}{\pi}\right)\sigma^{(1)}. \quad (53)$$

The last term comes from the renormalization of the strong coupling constant in the $O(\alpha_s)$ cross section; we need only keep the $-N_f/6$ term in the beta function. Adding these contributions, we obtain

$$\frac{\sigma^{(2)}}{\sigma_0}=N_f\left(\frac{\alpha_s}{\pi}\right)^2\left[\delta_{j,2}\left(\frac{(2.6\pm 4.6)\times 10^{-6}}{\epsilon^3}+\frac{(1.4\pm 5.5)\times 10^{-5}}{\epsilon^2}-\frac{(3.1\pm 5.2)\times 10^{-4}}{\epsilon}+1.799\pm 0.003\right) +\delta_{j,3}\left(\frac{(-0.5\pm 2.6)\times 10^{-4}}{\epsilon}-1.917\pm 0.017\right)+(1.456\pm 0.002)\times 10^{-3}\delta_{j,4}\right]. \quad (54)$$

As we see, the divergences associated with various pieces disappear, with small remnants consistent with the integration errors. The cancellation occurs independently for the 2 and 3 jet cross sections, as required. Finally, adding together the 2, 3, and 4 jet cross sections, we obtain the total hadronic cross section

$$\frac{\sigma^{(2)}}{\sigma_0}=(-0.117\pm 0.003)N_f\left(\frac{\alpha_s}{\pi}\right)^2, \quad (55)$$

which agrees with the known analytic result [14]:

$$\frac{\sigma^{(2)}}{\sigma_0}=\left(\frac{2}{3}\zeta_3-\frac{11}{12}\right)N_f\left(\frac{\alpha_s}{\pi}\right)^2=-0.115\ \ N_f\left(\frac{\alpha_s}{\pi}\right)^2. \quad (56)$$

Again, the integration error of the finite piece can be improved with a more sophisticated numerical integration technique. We conclude that our method can be applied successfully to compute differential quantities.

## VI. CONCLUSIONS

We have presented a new technique for computing double real emission corrections at NNLO. Our method uses sector decomposition of the four particle phase space, together with an expansion in plus distributions, to extract the phase-space singularities without any analytic integrations, and preserves the exact kinematics of the partonic event. The expressions for the matrix elements obtained with this approach can be used as building blocks for Monte Carlo event generators.

A phenomenologically attractive feature of our method is that constraints on the final-state phase space, including various jet algorithms, can be implemented simply. This makes it possible to study radiative corrections to quantities of direct experimental relevance. The method is completely automated, and flexible. It can be applied to any QCD or electroweak process with massless particles in the final state, where the singularities from double-real unresolved radiation must be extracted.

We have illustrated our approach using $e^+e^-\rightarrow$ jets at $O(\alpha_S^2)$ as an example. We have considered the most complicated phase space integrals that appear. We have explicitly checked our results for those integrals by performing an inclusive numerical integration over the phase space and comparing with analyting results obtained by using the unitarity method. We have also demonstrated that our method is capable of calculating differential quantities at NNLO by deriving the $N_f$ dependent contributions to the $O(\alpha_S^2)$ cross section for $e^+e^-\rightarrow$ jets; this includes $e^+e^-\rightarrow 2$ jets at NNLO, $e^+e^-\rightarrow 3$ jets at NLO, and $e^+e^-\rightarrow 4$ jets at LO. The $1/\epsilon$ poles were cancelled numerically, and the finite piece for the inclusive cross section agrees with results in the literature.

Results for the non-$N_f$ contributions will be given elsewhere. We have already presented here the calculation of the most difficult contributions needed for these terms. In addition, the bookkeeping of the various sector decompositions, and the numerical integrations, have already been addressed here.

While a direct application of our formalism to more complicated phase spaces is a viable option, one could also use it profitably in conjunction with a dipole formalism. Sector decomposition can be applied to the dipoles to extract the $1/\epsilon$ singularities they contain, without the need for an analytic integration. The remainder can be integrated numerically. Sector decomposition of the finite terms should also improve the numerical stability of the dipole approach.

There are several possibilities to develop the method further. It is interesting to investigate its direct application to $1\rightarrow 5$ processes. It is also important for many applications to study the factorization of the phase space when massive particles appear in the final state. Although the parametrization of the phase space is certainly more complicated in those cases, we do not anticipate any significant limitations of the method. We also expect that the number of required sector

decompositions will be reduced in the presence of massive particles.

Our method is a promising new technique for computing real radiation contributions to NNLO cross sections, and allows to obtain phenomenological results vital for the future of precision high energy physics. We look forward to the application of our method to many important collider physics processes.

*Note added*. While this paper was being completed, a new paper appeared which discusses the application of sector decomposition to inclusive phase space integrals [18].

## ACKNOWLEDGMENTS

The work of C.A. is supported by the DOE under grant number DE-AC03-76SF0515. The work of K.M. is partially supported by the DOE under grant number DE-FG03-94ER-40833 and the Outstanding Junior Investigator program through grant No. DE-FG03-94ER40833. The work of F.P. is supported by NSF grants P420D3620414350 and P420D3620434350. F.P. thanks the University of Hawaii at Manoa for kind hospitality during the completion of this work.

[1] For a review, see T. Gehrmann, hep-ph/0310178, and references therein.
[2] D.A. Kosower, Phys. Rev. D **67**, 116003 (2003).
[3] D.A. Kosower, Phys. Rev. Lett. **91**, 061602 (2003).
[4] S. Weinzierl, J. High Energy Phys. **03**, 062 (2003).
[5] S. Weinzierl, J. High Energy Phys. **07**, 052 (2003).
[6] R.K. Ellis, D.A. Ross, and A.E. Terrano, Nucl. Phys. **B178**, 421 (1981).
[7] W.T. Giele and E.W.N. Glover, Phys. Rev. D **46**, 1980 (1992).
[8] K. Fabricius, I. Schmitt, G. Schierholz, and G. Kramer, Phys. Lett. **97B**, 431 (1980).
[9] F. Gutbrod, G. Kramer, and G. Schierholz, Z. Phys. C **21**, 235 (1984).
[10] S. Catani and M.H. Seymour, Nucl. Phys. **B485**, 291 (1997); **B510**, 503(E) (1997).
[11] T. Binoth and G. Heinrich, Nucl. Phys. **B585**, 741 (2000).
[12] G. Heinrich, Nucl. Phys. B (Proc. Suppl.) **116**, 368 (2003).
[13] T. Binoth and G. Heinrich, Nucl. Phys. **B680**, 375 (2004).
[14] R.K. Ellis, W.J. Stirling, and B.R. Webber, *QCD and Collider Physics* (Cambridge University Press, Cambridge, England, 1996).
[15] S.G. Gorishnii, S.A. Larin, L.R. Surguladze, and F.V. Tkachov, Comput. Phys. Commun. **55**, 381 (1989).
[16] R.J. Gonsalves, Phys. Rev. D **28**, 1542 (1983).
[17] G. P. Lepage, ''Vegas: An Adaptive Multidimensional Integration Program,'' Report No. CLNS-80/447.
[18] A. Gehrmann-De Ridder, T. Gehrmann, and G. Heinrich, hep-ph/0311276.